UNIVERSITY OF CALIFORNIA SAN DIEGO

Optogenetic control of the medial septal area leads to reliable pacing of theta oscillations in the medial prefrontal cortex but the endogenous ~4-5 Hz oscillations remained unaffected

A Thesis submitted in partial satisfaction of the requirements

for the degree Master of Science

in

Biology

by

Yudi Hu

Committee in charge:

Professor Stefan Leutgeb, Chair
Professor Jon Christopher Armour
Professor Jill Leutgeb

2021

The thesis of Yudi Hu is approved, and it is acceptable in quality and form for publication on microfilm and electronically.

University of California San Diego

2021

DEDICATION

I humbly dedicate this thesis to my grandparents for their unconditional love, to my parents for their sacrifices and trust in me, and to my friends for being my biggest cheerleaders of all time.

Above all, to Almighty God who has given me the guidance, enlightenment, strength, and wisdom that I needed to get through the darkest times.

TABLE OF CONTENTS

LIST OF ABBREVIATIONS

HpC	Hippocampus
mPFC	medial Prefrontal Cortex
MSA	Medial Septal Area
PV+	Parvalbumin- positive
LFP	Long Term Potentiation
AVV	Adeno Associated Virus
AP	Anterior Posterior
ML	Mediolateral
DV	Dorsoventral
PFA	4% Paraformaldehyde
PBS	Phosphate Buffered Saline
ChR2	Channelrhodopsin-2
eYFP	Yellow Fluorescent Protein
GFP	Green Fluorescence Protein

LIST OF FIGURES

LIST OF TABLES

ACKNOWLEDGEMENTS

I would like to first acknowledge Dr. Stefan Leutgeb, the principal investigator for the lab in which I completed my master's thesis. Thank you for serving as the chair of my committee and helping me along the journey. From reading scientific literatures to writing about my own research, your patience and expertise not only helped me accomplish this project but also taught me how to think and communicate as a scientist. Thank you for your continued support and encouragement.

I would also like to acknowledge Dr. Chris Armour for serving on my committee. I never thought I could act as a researcher until the day I took BIPN 105 Animal Physiology Lab with you. I will never forget the struggles of plotting figures using Kaleidagraph and the all-nighters I pulled to finish the lab reports. But I will forever cherish all the guidance and knowledge you have taught me, Dr. Armour.

I would like to acknowledge Dr. Jill Leutgeb as well for being part of my committee. Your challenging questions always helped me understand my project better. Thank you for pushing me to think more critically.

I would like to thank everyone who I have interacted with in the Leutgeb Labs. I would like to thank Thao Tang, who is more than a lab mate but also a dear friend of mine. Thank you for all your morning calls and gentle pinches to make sure I show up and stay awake in my 8am class. Also, thank you for teaching me how to use the microtome over the phone even after you have left the lab. I would also like to thank Antonia Schonwald, Maylin Fu and Marina Jaramillo for being the best lab managers one could ever have. Thank you for never failing to show me where things were when I was lost in the maze of wet lab (like my mice on a figure-8 maze). I always feel so lucky that I am not in this BSMS program by myself. I would like to thank my

BSMS buddies Ameen Khan and Adeh Vartanian. Thank you for your continued help since the day we embarked on this journey together. I would also like to thank everyone who has chatted with me in the office, come to my lab meetings, or said hi to me in the hallway. You all made my experience at the Leutgeb Lab memorable.

I must also thank my family and friends who offered me constant support in this process. Thank you, Abi, Jenny, Nitika and Kriti for being part of my life. College is like a roller coaster ride and you all are the seat belt on that roller coaster. Without you all, gravity would have already dragged me down.

Finally, I would like to acknowledge Sunandha Srikanth. I am so honored to have you as my mentor ever since the first day I joined the Leutgeb Lab. I am not the smartest student but you have always been the most patient teacher. Like our mice who often forget the rule of alternation, I sometimes would forget even the most basic things. But you have always been so patient with all my spam texts and explained to me over and over again. There were times when I felt like a complete failure but you always faced the problems with me and tried your best to help me out. Now instead of panicking, I think I have learned how to troubleshoot when problems occur. And I learned that from you. I never thought I could finish a master's thesis and I would have been right if you had not been here. Thank you for having trust in me and pushing me move forward along the journey. Thank you for being so supportive both in and outside of lab. By the way, until this day I am still grateful that you kept me as a volunteer even after knowing I have never read Harry Potter.

This thesis is currently being prepared for submission of publication of the material by Srikanth, Sunandha.; Hu, Yudi.; Leutgeb, Jill K.; Leutgeb, Stefan. The author of this thesis will be a co-author of the publication.

ABSTRACT OF THE THESIS

Optogenetic control of the medial septal area leads to reliable pacing of theta oscillations in the medial prefrontal cortex but the endogenous ~4-5 Hz oscillations remained unaffected

by

Yudi Hu

Master of Science in Biology

University of California San Diego, 2021

Professor Stefan Leutgeb, Chair

The hippocampus (HpC) and medial prefrontal cortex (mPFC) are known to be crucial for working memory. Both of the two brain regions exhibit prominent theta oscillations (7-9 Hz) which coordinate neuronal activity between the HpC and mPFC in working memory.

Hippocampal theta oscillations are generated and paced by GABAergic neurons in the medial septal area (MSA), and optical stimulation of the GABAergic septal neurons can be used to modulate hippocampal theta oscillations. In our study, we found that hippocampal and mPFC theta oscillations shifted to the stimulation frequency with optical stimulation in the MSA. In addition, the power of theta oscillations in mPFC and the coherence of the oscillations between the mPFC and HpC also increased at the stimulation frequency. However, we found that mPFC power and mPFC-HpC coherence of endogenous ~4-5 Hz oscillations remained unaffected by septal stimulation. We also examined the effects of MSA stimulation on performance of a figure-8 maze alternation task and no behavioral improvements or impairments were observed.

INTRODUCTION

The hippocampus is critical for spatial working memory

The hippocampus (HpC) and adjacent areas in the medial temporal lobe are known to be important for declarative memory (Scoville and Milner, 1957; Eichenbaum, 2000). This was first discovered in 1954, when Patient H.M. underwent a bilateral medial temporal lobectomy that removed the HpC, amygdala, and the adjacent parahippocampal gyrus (Scoville and Milner, 1957; Squire 2008). After the medial temporal lobe removal, patient H.M. was not able to recognize hospital staff nor remember daily events, indicating a loss of episodic memory, a type of declarative memory that requires learning, storing and retrieving of unique experiences in daily life (Milner et al., 1968; Squire 2008). Anatomical studies conducted later confirmed the structure responsible for H.M.'s memory deficit was the medial temporal lobe (MTL) which consists of the HpC and the adjacent perirhinal, entorhinal, and parahippocampal cortices (Squire and Zola-Morgan, 1991). These findings suggest that one of these structures or a combination thereof is critical for episodic memory (Squire and Zola-Morgan, 1991; Dickerson and Eichenbaum, 2010). To examine the contribution of a combined lesion of the MTL compared to a selective hippocampal lesion to memory, Andre Rey and Paul-Alexandre Osterrieth proposed and standardized the Rey-Osterrieth complex figure test. It examined memory function in patients with different degrees of MTL damage. Patients with either large MTL damage, only hippocampal damage, or no brain damage were presented with a complex figure. Five to ten minutes after copying the figure, the patients were asked to reproduce it (Reed and Squire., 1998). All groups were able to copy the figure accurately but after a 5-10 min delay the group with entire MTL damage and the group with only hippocampal damage were not able to reproduce the figure. In addition, the MTL lesioned group demonstrated a more severe memory

impairment than the hippocampal damaged group. It could thus be concluded that the HpC is needed and critical for episodic memory in humans, but that memory deficits become progressively more severe with larger lesions of the MTL.

While early studies such as the patient H.M case study and the Rey Osterrieth test have provided valuable information on what brain regions support episodic memory, studies involving human participants have brought about many limitations such as challenges in recording neuronal activities and ethical concerns. Therefore, researchers adopted animal models in memory studies. This raises another problem, however. Though the mechanisms underlying memory deficits after hippocampal damage can be effectively studied in animal models, the use of rodent models is accompanied by the difficulty to study complex forms of memory, including episodic memory. Episodic memory occurs when subjects learn a task in one trial, which is challenging for rodents to achieve. Scientists therefore designed behavioral tasks that partially resemble episodic memory, using either spatial memory tasks or more complex episodic-like memory tasks to assess learning in rodents.

A commonly used task that is thought to mimic the "what" and "where" components of episodic memory is the Morris Water Maze task (Morris et al., 1982). In this task, rats are placed in a cloudy pool where they had to locate a hidden platform to successfully escape from the water. The pool is divided into quadrants and the one where the hidden platform is located is called the target quadrant. If the animal spends significantly more time exploring in the target quadrant compared to the other quadrants, it indicates that they have learned in which area the hidden platform is located (Morris et al., 1982). Compared to control animals, hippocampus lesioned animals spent significantly less time in the target quadrant, demonstrating the importance of the HpC for this memory task (Morris et al., 1982). However, this experimental

setup has a shortcoming such that it requires multiple training trials, making the memory resemble a reference memory for a place rather than memory for a single learning episode.

To decrease the reliance of memory tasks on multiple training trials, tasks with learning from one or few instances have been designed. These tasks better address the episodic memory components and are referred to as episodic-like memory tasks. One example of such a task is the paired-associate learning task in which rats are presented with an odor in a start box on the side of an arena which consists of 6 sand wells (Tse at al., 2006). The animals are then trained to forage into the arena and find the well containing the same odor as they are presented with in the start box. Training is achieved by giving the animals a food reward when they identify the correct well (Tse at al., 2006). Performance is analyzed by comparing the time the rats spend digging at incorrect compared to correct sand wells. Rats are considered to have learned the task if they spend significantly more time digging at the correct well (Tse et al., 2006). Hippocampus lesioned rats spend similar amounts of time digging in both correct and incorrect wells such that the difference is at chance level (Tse et al., 2006). This indicates behavioral performance is impaired by the absence of the HpC, suggesting episodic-like memory in rodents is hippocampal dependent.

While the paired-associate learning task is effective at addressing the episodic-like component of memory, such complex tasks are not ideal for electrophysiological recordings, where repeated trials are required to identify neuronal activity patterns. Therefore, instead of using behavioral tasks that study episodic-like memory, scientists designed simpler tasks to examine working memory, a type of short-term episodic memory (Baddeley, 1992). Ainge and Wood utilized a T-maze alternation task to study spatial working memory in rodents (Ainge et al., 2007; Wood et al., 2000). Rats were trained to make alternating left and right turns on a T-

shaped maze. A hippocampal lesion surgery was performed after the animals have learned the task (Ainge et al., 2007; Wood et al., 2000). Post-surgical testing showed that rats with hippocampal damage performed significantly worse than the controls when they were asked to stay in a delay zone for either 2 or 10 seconds before turning. Additionally, the performance impairment was shown to be more severe with a longer delay interval (Ainge et al., 2007). Besides the T-maze alternation task, figure-8 maze alternation and W maze tasks are also often used for assessing spatial working memory (Frank et al., 2000; Sabariego et al., 2019). In the Sabariego et al. study, when delays were introduced to the figure-8 maze task, rats with a combined medial entorhinal cortex (mEC) and hippocampal lesion performed worse than mice with only an mEC lesion. This indicates that the HpC can partially support working memory when mEC is damaged (Sabariego et al., 2019). In both figure-8 and T-maze alternation tasks, longer delays lead to more severe memory deficits, indicating the HpC becomes more important for storing information as the delay intervals become longer (Sabariego et al., 2019; Ainge et al., 2007; Wood et al., 2000). In the continuous version of spatial working memory tasks, however, the performance of hippocampal lesioned group is not significantly different from that of the control group (Sabariego et al., 2019; Wood et al., 2000). Even when running on the maze without delays, the animals still need to retain information for a short period before making a choice to turn left or right. This suggests that there are other brain structures that can compensate for the absence of the HpC and support spatial working memory over very brief intervals.

The medial prefrontal cortex can compensate for hippocampal damage in working memory with short delays

In addition to the HpC, medial prefrontal cortex (mPFC) is also a critical region for episodic memory as shown by mPFC lesion studies. In a delay Y-maze alternation task, rats learned to choose alternating arms between trials (Yang et al., 2014). In this task, the mPFC lesioned group performed significantly worse than the control group (Yang et al., 2014). Similarly, Shaw and Aggleton trained rats in a T-maze delayed non-matching-to-sample spatial task. In their experiment, rats with mPFC lesions performed significantly worse than controls (Shaw and Aggleton., 1993). Memory deficits in the prefrontal-lesioned mice have been found to be specifically related to the prelimbic region of mPFC which receives projections from the HpC through the fornix (Shaw and Aggleton., 1993). These studies showed the necessity of mPFC in working memory and also suggested that connections between mPFC and HpC might be critical for spatial memory. In a study that directly compared prefrontal and hippocampal contributions to working memory, rats were first placed on a study arm in an eight-arm maze, after which they were confined in the central platform for a delay period. The animals had access to both an unvisited choice arm and a visited study arm after the delay period. To receive a food reward, they needed to choose the unvisited arm (Lee and Kesner, 2003). During a short delay period, inactivating mPFC or dorsal HpC caused an initial deficit in short-term memory while performance improved over time to a normal value. This indicates that the dorsal HpC and mPFC process spatial working memory in parallel and can compensate for each other (Lee and Kesner, 2003). However, when the delay period was increased, the hippocampal lesion led to severe memory impairments despite the presence of an intact mPFC. This indicates that the

mPFC compensatory mechanism failed to function with long delay periods (Lee and Kesner, 2003).

In addition to the studies that combined lesions with behavioral testing and found a similar function for mPFC and HpC in working memory tasks, anatomical studies that examined connections between mPFC and the HpC found excitatory monosynaptic projections from the hippocampal CA1/Subiculum area to the prefrontal regions (Amaral and Witter, 1989). The mPFC projects back to dorsal CA1 via indirect routes, one via the entorhinal cortex and the medial dorsal thalamic nuclei and the other via the nucleus rotundus (Rajasethupathy et al., 2015; Dolorfo and Amaral, 1998). In combination, the lesion studies and anatomical findings suggest that the circuits that includes mPFC and HpC support working memory, which motivates further studies to identify the physiological mechanism that couples these brain regions.

Theta oscillations coordinate neuronal activity between mPFC and the HpC

Behavioral studies revealed that the HpC and mPFC are crucial brain regions in working memory. To study the physiological mechanism that couple these two regions, it is important to understand the neuronal activity patterns during working memory. Brain oscillations are known to coordinate neuronal activities across different brain regions and mediate memory functions (Fries, 2009; O'Neill et al., 2013; Colgin, 2011). Three main oscillatory patterns exist in the HpC: theta oscillations, gamma oscillations, and sharp wave ripples (Colgin, 2011). Among them, hippocampal theta oscillations (4-12Hz) have been shown to be an important factor in episodic memory formation (Vanderwolf, 1969; O'Keefe and Recce, 1993; Backus et al., 2016). On the other hand, prominent theta oscillations are also observed in mPFC in local field potential (LFP) recordings (Siapas et al., 2005; Brincat and Miller, 2015). Simultaneous LFP recordings in

the HpC and mPFC have shown increased theta coherence between dorsal HpC and mPFC in a spatial working memory task, indicating that theta rhythm is the mediator of neuronal activities in the HpC and mPFC (Siapas et al., 2005; O'Neill et al., 2013). Besides theta oscillations, mPFC also exhibits an endogenous 4Hz oscillation which was shown to have an increase in power during a working memory task (Fujisawa and Buzsaki., 2011). Both theta and the 4 Hz oscillations in the mPFC are studied in my thesis.

Medial septal area generates theta oscillations in the HpC

To study the hippocampal-prefrontal theta synchrony, it is important to understand the mechanisms that generate theta oscillations. Theta oscillations in the HpC are thought to be dependent on neuronal activities in medial septal area (MSA) which includes medial septal nucleus and the diagonal band of Broca (Winson et al., 1978; Mitchell et al., 1982). Lesion studies demonstrated that hippocampal theta oscillations were abolished when MSA was damaged (Mitchell et al., 1982). To study the relationship between hippocampal theta oscillation and spatial working memory, Winson first trained rats to perform on a circular maze and then lesioned the medial septal nucleus, which eliminated hippocampal theta oscillations (Winson, 1978). He also observed severe memory impairments in the lesioned animals that lost hippocampal theta oscillations. Based on these studies, researchers concluded that MSA generates hippocampal theta and the loss of hippocampal theta leads to memory deficit (Mitchell et al., 1982; Winson, 1978).

Modulation of hippocampal theta oscillations

Knowing that MSA generates theta oscillations in the HpC, scientists have used different methods to inactivate or manipulate hippocampal neuron firing patterns via the MSA. Lidocaine inactivates neuron activities by blocking sodium channels. It is proven to have a transient and reversible nature which is ideal for inactivating a brain region in spatial tasks (Tehovnik and Sommer., 1997, Rossi et al., 2012; Hannesson et al., 2003). Lidocaine injection in the MSA has been shown to inactivate neuron activities and therefore impair spatial working memory (Poucet and Buhot, 1994). On the other hand, Zutshi et al utilized an optogenetic approach aiming to achieve high-fidelity control of hippocampal theta rhythm in behaving mice. Optogenetic technology can target specific cell types and allows for reversible inhibition or activation of cells in a defined brain region (Ji and Neugebauer., 2012). In their experiment, Zutshi et al specifically targeted GABAergic parvalbumin (PV)-positive medial septal neurons, which are known to be crucial in generating hippocampal theta oscillations, with Channelrhodopsin-2 virus. They monitored LFP and pyramidal neurons spiking in the CA1 area of the HpC when optical stimulation was delivered (Zutshi et al., 2018). Their study showed optogenetic stimulation of the medial septal PV neurons can supersede the endogenous hippocampal theta oscillations (Zutshi et al., 2018).

Although previous studies have indicated reliable pacing of hippocampal LFP by optogenetic control of the medial septal neurons (Zutshi et al., 2018), it remains unknown how optogenetic stimulation of medial septal neurons affects mPFC theta oscillations and hippocampal-prefrontal coherence. In this study we would like to explore the effects of optogenetic stimulation in the MSA on mPFC theta oscillations and the coordination between the mPFC and HpC in a figure-8 maze alternation task. The following research questions will be

asked: (1) whether manipulations of theta oscillations in the MS jointly affect the coordination of theta oscillations between the HpC and mPFC. (2) How these manipulations affect performance in a figure-8 maze spatial alternation task.

CHAPTER I: METHODS

Subjects

Genetically modified mice that selectively express CRE in parvalbumin neurons (129p2-Pvalbtm1(cre)arbr/j, Jackson Labs) were used in this study. The study's subjects consisted of 6 male and 7 female PV-Cre mice, which were 3-6 months old and weighed at least 20 grams. All mice were housed in a reverse 12 hr dark/light cycle. Lights were turned off from 8:00 am to 8:00 pm. Mice were restricted to 85% of their *ad libitum* weight and given full access to water during behavior training and recording. Experimenters weighed the animals every day to monitor their health. *Ad* libitum food was provided before the mice underwent an implantation surgery and during surgery recovery period. All procedures were conducted in accordance with the University of California, San Diego Institutional Animal Care and Use Committee. All experiments conducted in this project followed the guidelines outlined by the National Institutes of Health (NIH) for the care and use of laboratory animals.

Behavioral Training

Apparatus. Mice were food restricted and trained on a figure-8 maze delayed alternation task (Figure 2A). The maze was 50 cm above the ground. The runways that formed the return and stem arms were 75 cm long, and the runways that formed choice arms were 25 cm long. All runways were 5 cm wide. The delay zone was on the first 25 cm of the stem and was created

with cardboard barriers. The maze was cleaned with water and dish soap after each mouse was tested on the maze. Animals were trained in several phases before being recorded in the final version of the behavioral task.

Habituation. In the first phase of this task, animals were habituated to the maze by freely exploring the maze and foraging for chocolate sprinkles (Betty Crocker) for 15 minutes. The animals were handled by the same experimenter throughout the experiments to ensure they were comfortable with the presence of the experimenter.

Forced continuous alternation. Mice were placed on the figure-8 maze with cardboard barriers placed on both ends of the central arm. Animals were forced to run continuously on the maze and make alternating left and right turns. A chocolate sprinkle was given to the animal in the reward zone of each return arm. Forced alternation lasted for 3 days and each training day lasted 20 minutes. By the end of the forced alternation training, animals were comfortable with running on the maze and eating the food rewards.

Continuous alternation. Barriers were removed from the central arm and animals were allowed to run continuously on the figure-8 maze for 60 trials per session. In order to receive a chocolate sprinkle reward, the animals needed to remember which arm they turned to in the previous trial and make an alternative turn in the following trial (Figure 2A). Trials were marked correct when the animals turned in the opposite direction compared to the previous trial. After the animals reached the criterion of >80% correct performance on 2 out of 3 consecutive days, they started delayed alternation training.

Delayed alternation. 2-second and 10-second delay intervals were introduced to the figure-8 alternation task. During each delay interval, cardboard barriers were placed at both ends of the delay zone, forcing the animal to stay in the delay zone until the delay period was over.

Once the cardboard barriers were removed from the delay zone, animals were allowed to run down the central arm and turn to either the left or right. A chocolate sprinkle reward was placed in the reward zone after each correct trial (Figure 1A). Each delayed alternation training session consisted of 60 trials which were divided into 6 blocks with 10 trials in each block. During the training sessions, the first block was always no delay, followed by a 2-second delay block and a 10-second delay block. The delay order was repeated twice in the 60-trial session so each session consisted of an equivalent number of no delay, 2-second delay, and 10-second delay trials. After the animals reached the criterion of >80% correct performance on 2 out of 3 consecutive days, they were prepared for an implantation surgery, during which a silicon probe was implanted in the medial prefrontal cortex (mPFC), an electrode in the CA1 region of the ipsilateral hippocampus, and an optic fiber over the medial septal area (MSA).

Retraining: After recovering from surgery, mice were retrained while being attached to a recording cable. The cable was connected to a Neuralynx adapter mounted on the ceiling that prevents the tether from getting tangled. The length of the tether cable was adjusted for each animal to facilitate its running. The position of the maze was also adjusted for each animal such that the animal makes unbiased left and right turns. Retraining lasted until the mice reached the criterion of >80% correct on 2 out of 3 consecutive days. The silicon probe was turned down 50 micrometers daily during the retraining phase.

Surgeries

Viral vector surgery. Viral vectors were injected into the MSA of PV-Cre mice that selectively express CRE in parvalbumin neurons. Mice were anesthetized with isoflurane (induction: 3%, maintenance: 1.5-2%) and mounted in a stereotaxic frame (David Kopf

Instruments, Model 1900). The scalp was cleaned and retracted using a midline incision and the skull was leveled between bregma and lambda. A hole was drilled above the MSA (AP: +1.0, ML: -0.7). The skull was then angled at a mediolateral angle of 10°. Using a glass pipette, a volume of 500 nL of viral vector was injected at each injection site in the MSA (DV: -4.8, -4.2) at a rate of 150 nL/min. We used one of two Cre-dependent viral vectors - AAV.EF1.DIO.ChR2.eYFP or AAV.EF1.DIO.eGFP. The experimental group consisted of mice expressing channelrhodopsin (ChR2) and the control group consisted of mice expressing a green fluorescent protein (GFP). The pipette was left in place for 10 minutes after each injection and retracted very slowly to prevent back flow of the virus. The incision site was sutured, and the mice were allowed to recover for a minimum of 5 days. Postoperative care was administered as needed.

Implantation surgery. Mice were anesthetized with isoflurane (induction: 3%, maintenance: 1.5-2%) and mounted in a stereotaxic frame (David Kopf Instruments, Model 1900). The scalp was cleaned and retracted using a midline incision and the skull was leveled between bregma and lambda. Five holes were drilled in the skull to attach anchor screws. A hole was drilled above the cerebellum to place the ground screw. An optical fiber was implanted over the MSA (AP: +1.0, ML: -0.7, DV: -3.7, angled 10° medio-laterally), a 32-channel silicon probe (Neuronexus Buzsaki32-H32_21mm probe) was implanted in the mPFC (AP: +2.0-2.6, ML: 0.4, DV: -0.6) and an electrode wire was implanted in the CA1 region of the hippocampus (AP: -1.9, ML: 2.0, DV: -1.8). The silicon probe was mounted on a movable drive (Cambridge nano-drive) for implantation. The implant was secured with Metabond and dental cement. Postoperative care was administered as needed and mice were allowed to recover for a minimum of 5 days.

Electrophysiological Recordings

The recording phase started after animals reached the criterion of the retraining phase. The silicon probe was connected to a preamplifier which forwarded signals to a digital Neuralynx recording system. Signals were filtered from 0.1 Hz to 8000 Hz, with an acquisition frequency of 32000 Hz. Before each recording session, signals of each channel were examined and the prefrontal channel with the least observed spikes was replaced by the hippocampus CA1 wire to record hippocampal LFP signals. The remaining 31 of the 32 channels recorded signals from the silicon probe in mPFC. LFP signals were obtained by offline filtering signals between 1 and 500 Hz using a customized Python script. Single cells were not analyzed as part of the thesis. A video camera was mounted on the ceiling above the maze and was connected to the Neuralynx video tracking system to monitor the animal's position. A 10-minute sleep session, in which animals were resting in the home cage, was performed before and after the behavioral task. Mice were tested for 60 trials in 6 blocks of 10 trials daily. Each delay was repeated in two blocks and the order of delay (no delay, 2-second delay, 10-second delay) for each recording session was randomized (Table 1). Laser stimulation was delivered on alternating 10-trial blocks with a 125 ms pulse interval (50% on-off cycle). In the recording phase, laser light was delivered to the MSA using a 473 nm wavelength Blue DPSS Laser System through an optic fiber patch cord (Doric Lenses, MFP_200/240/1100-0.22_10m_FC-ZF1.25(F), 200 μm core, 0.22 NA) to an optical fiber. 4 Hz, 8 Hz and 12 Hz stimulation frequencies were used in the recording sessions and the order of stimulation frequencies was randomized for a subset of the animals (Table 1). 11 out of the 13 animals included in the analysis underwent 15 recording sessions with 5 sessions per stimulation frequency. Two animals completed fewer than 15 sessions due to too many broken channels of the implanted silicon probe. The silicon probe was turned down by 50

micrometers after each recording session. After all recording sessions were completed, animals were given *ad libitum* food.

Table 1. Example of randomization of delay intervals and stimulation frequencies. In the electrophysiological recording phase, the order of delay intervals was randomized for all animals and the order of stimulation frequencies was randomized for a subset of animals.

	S28	
Day	Frequency	Delay
1	12Hz	10s 2s 0s
2	4Hz	0s 10s 2s
3	8Hz	2s 10s 0s
4	4Hz	2s 0s 10s
5	8Hz	10s 0s 2s
6	12Hz	0s 2s 10s
7	8Hz	2s 10s 0s
8	4Hz	10s 2s 0s
9	12Hz	2s 10s 0s
10	4Hz	0s 2s 10s
11	8Hz	10s 0s 2s
12	12Hz	0s 10s 2s
13	8Hz	2s 0s 10s
14	12Hz	10s 2s 0s
15	4Hz	0s 10s 2s

Histology

Mice were perfused with 0.1 M phosphate-buffered saline (PBS) followed by 4% paraformaldehyde in PBS solution. Brains were post-fixed for 24 hours in 4% paraformaldehyde and then cryoprotected in 30% sucrose solution for 2 days. After that, mouse brains were sectioned into 40 μm coronal slices throughout the extent of the MSA, mPFC, and hippocampus using a microtome. The brain slices were mounted on electrostatic slides and cover-slipped with DAPI. Slides were imaged using a virtual slide microscope (Olympus, VS120). Histology scans

were used to confirm that the optic fiber was implanted over the MSA, the silicon probe was placed in the mPFC, and the electrode was placed in the hippocampus CA1 region.

Data Analysis

Statistical analysis was performed using Matlab and Microsoft Excel. The performance of the animals was averaged across all the sessions of the same stimulation frequency. Paired t-tests were performed across all delay intervals for both ChR2 and control animals to evaluate the difference in performance accuracy between stimulation turned on and stimulation turned off trials. P values obtained from the paired t tests were corrected for multiple comparisons using Holm-Bonferroni correction. LFP analysis was performed using customized Python 3 and Matlab script. Pacing scores analysis was performed using Wilcoxon rank sum tests followed with Holm-Bonferroni correction. LFP power and mPFC-HpC coherence analyses were performed using Wilcoxon signed rank tests followed with Holm-Bonferroni correction.

CHAPTER II: RESULTS

Expression of AAVs in the MSA and placement of electrodes in HpC and in mPFC were confirmed

To determine how the effects of manipulation of hippocampal theta oscillation on mPFC theta oscillations, we used an optogenetic approach that has been shown to be effective in previous studies (Zutshi et al., 2018). Because hippocampal theta oscillations are known to be generated and paced by GABAergic parvalbumin (PV)-positive medial septal neurons, we injected an adeno-associated viral vector (AAV) expressing channelrhodopsin-2 (ChR2) in the MSA of PV-Cre transgenic mice. For the control group, AVV expressing a green fluorescent protein (GFP) was injected in the MSA of PV-Cre transgenic mice (Figure 1A). An optic fiber was placed in the MSA to activate PV-positive neurons expressing ChR2 and pace hippocampal theta rhythm with the delivery of blue light of different frequencies (Figure 1A). mPFC LFP signals were collected from a 32-channel silicon probe and it was confirmed all recording sites in each mouse were located in the prelimbic and infralimbic regions of mPFC (Figure 1B). An electrode wire implanted in hippocampus was used to collect hippocampal LFP signals (Figure 1C).

Mouse brains were sectioned into 40 μm coronal slices for the MSA, mPFC, and HpC using a microtome. Brain slices were stained with DAPI, a counterstain used to stain cells and make distinctions between different tissues clearer. The detection of GFP in the MSA confirmed that the injection was placed at a site where it broadly infected medial septal neurons and at the constructs were selectively expressed in the MSA (Figure 1A). The shanks of the silicon probes were dyed with DiI, which could be detected with fluorescence microscopy in the mPFC and confirm placement of the shanks at the intended target site. The electrode track in the HpC was

sufficiently prominent to be detected with light microscopy in sections through the HpC, and the electrode wire tracks were confirmed to be placed in the hippocampal CA1 region (Figure 1B-C).

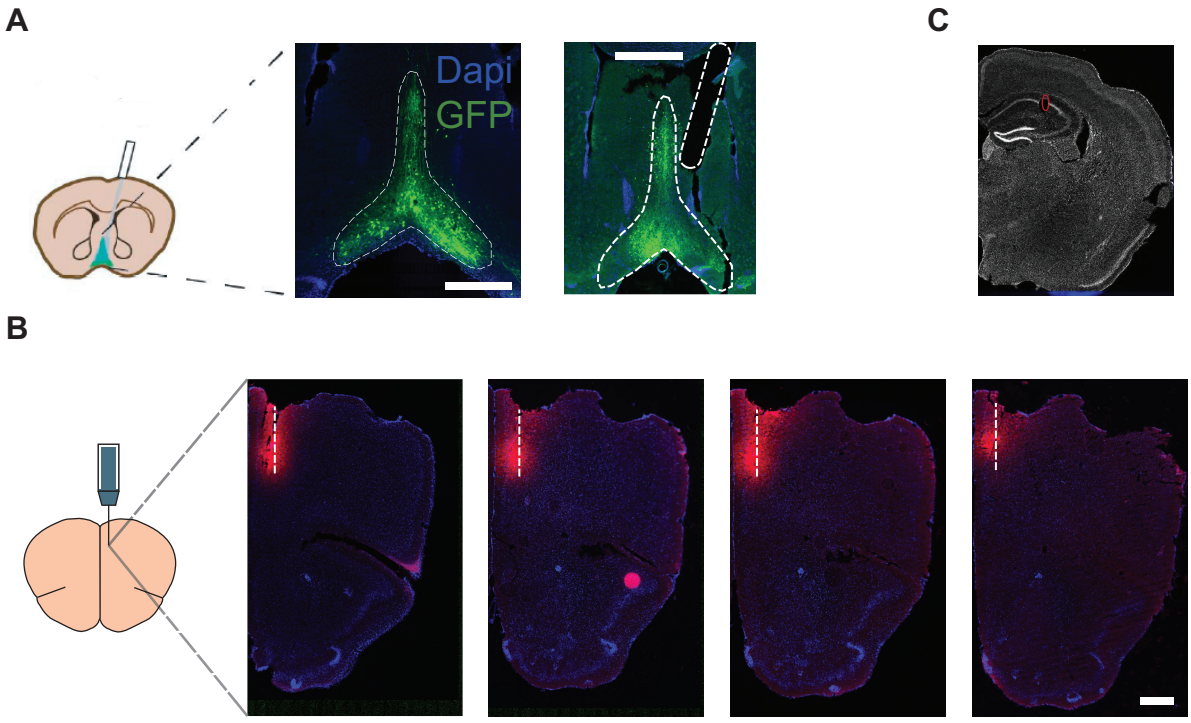

Figure 1. Viral expression and optic fiber tracks in the MSA, silicon probe tracks in mPFC, and electrode tracks in HpC were visualized in histological material. (A) AAV vectors that were injected into the MSA of PV-Cre transgenic mice expressed either ChR2-GFP or GFP. The MSA and the track by the optic fiber adjacent to the MSA are indicated by the white dash lines. Scale bar is 500 µm. (B) The 32-channel silicon probe was coated with DiI to confirm its placement in histological material. DiI staining is shown in red, and stippled lines represent the tracks of the silicon probe. In the mouse that is depicted, all tracks ended in the prelimbic region of mPFC, but other mice also included recording sites the infralimbic region. Scale bar is 500 µm. (C) An electrode wire was implanted in the hippocampal CA1 region to collect hippocampal LFP signals. The electrode tip is highlighted with a red circle.

Figure 2. Optogenetic stimulation of MSA PV neurons paced hippocampal LFP oscillations in a spatial alternation task. (A) Mice were trained and tested in a figure-8 maze alternation task. They were rewarded when choosing the opposite arm compared to the previous trial and not rewarded when choosing the same arm on consecutive trials. (B) Stimulation was turned off for the first block of a daily recording session and was turned on every other block. Each block consisted of trials with either no delay, 2-second delay, or 10-second delay, and each delay condition was repeated twice in a recording session. (C) Hippocampal LFP traces when 4 Hz, 8 Hz and 12 Hz stimulation was turned on and off. Black and colored traces are theta-filtered signals. Grey traces are unfiltered signals. Scale bar is 0.2s. (D) The predominant LFP frequency was measured every 2 s, and histograms shows relative frequency of the measured predominant hippocampal oscillation frequencies when stimulation was turned on (colored) or off (grey) in ChR2 animals. (E) The pacing score is the peak relative frequency [in the stimulation range (± 1Hz) during stimulation] from the histograms of predominant oscillation frequencies (as shown for example sessions in D). The summary plot shows the pacing score of HpC channels in ChR2 animals (colored dots and squares) and control animals (grey dots and squares). Pacing score is plotted by sessions (dots) or as the average over all sessions per animal (squares). Pacing score = Peak proportion.

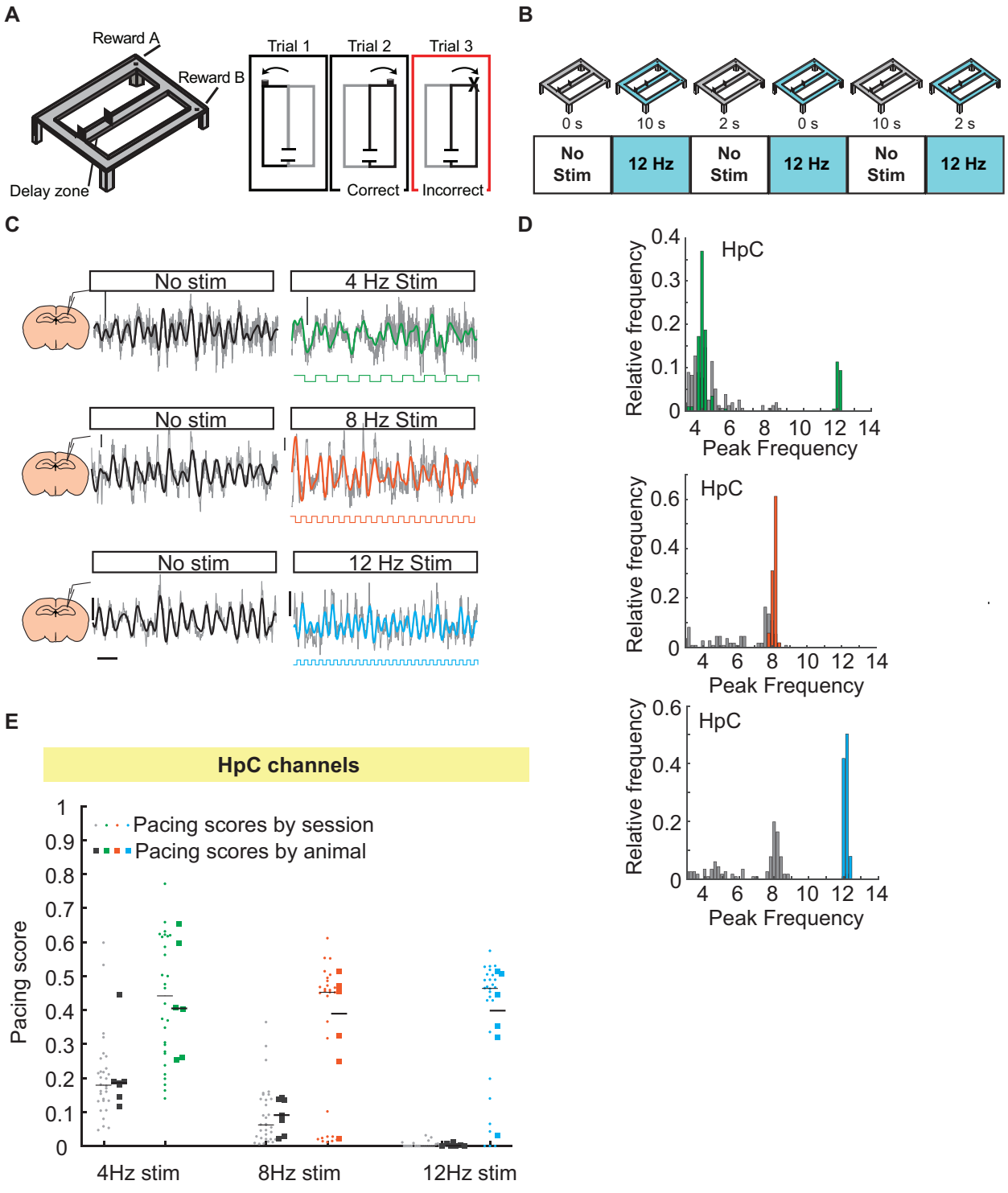
A
Reward A
Reward B
Delay zone
Trial 1
Trial 2
Trial 3
Correct
Incorrect
B
0 s
10 s
2 s
0 s
10 s
2 s
No Stim
12 Hz
No Stim
12 Hz
No Stim
12 Hz
C
No stim
4 Hz Stim
No stim
8 Hz Stim
No stim
12 Hz Stim
D
HpC
Relative frequency
Peak Frequency
HpC
Relative frequency
Peak Frequency
HpC
Relative frequency
Peak Frequency
E
HpC channels
Pacing scores by session
Pacing scores by animal
Pacing score
4Hz stim
8Hz stim
12Hz stim

Oscillations in the HpC and mPFC were paced by optical stimulation in the MSA

As described in the methods section, both ChR2 and control mice performed a figure-8 maze alternation task with stimulation turned on during every other block of 10 trials (Figure 2A-B). We modulated hippocampal theta rhythm by stimulating the septal PV neurons at frequencies of 4 Hz, 8 Hz and 12 Hz, which are below, within and above the endogenous theta range respectively (Figure 2A-B). As expected from previous studies, hippocampal theta oscillations shifted during rhythmic MSA stimulation from the endogenous frequency of ~7-9 Hz to the stimulation frequency (Figure 2C). Time-frequency spectra of hippocampal LFP were generated for each no stimulation and stimulation block with 0 second delay. The predominant oscillation frequency was measured for every 2-second intervals throughout the no stimulation and stimulation blocks. Histograms of these predominant frequencies were constructed for the no stimulation and stimulation block for each stimulation frequency. For ChR2 animals, during blocks with stimulation on, there was a peak in the histogram around the stimulation frequency. We defined pacing scores to determine the efficiency of pacing. The pacing score for each recording session was defined as the peak relative frequency in the histogram within a ± 1Hz range of the stimulation frequency (Figure 2E). ChR2 injected animals exhibited significantly higher pacing scores compared to the control animals (4 Hz: $p < .01$, $Z = -14.8$, Wilcoxon Rank Sum Test; 8 Hz: $p < .01$, $Z = -12.5$, Wilcoxon Rank Sum Test; 12 Hz: $p < 0.01$, $Z = -26.6$, Wilcoxon Rank Sum Test), indicating the successful pacing of oscillations in the HpC by all three stimulation frequencies. (Figure 2E).

We also examined the effects of optical stimulation of septal PV neurons on mPFC theta oscillations. Similar to hippocampal theta oscillations, mPFC theta oscillations were paced at the stimulation frequency when stimulation was delivered to the MSA (Figure 3A). Histograms of

the predominant frequencies in mPFC showed distributions that were clustered at the stimulation frequencies, indicating successful pacing of mPFC oscillations by 4 Hz, 8 Hz and 12 Hz optical stimulation in the MSA (Figure 3B). The pacing scores of mPFC oscillations were calculated using the same equation as for hippocampal oscillations. At all three stimulation frequencies, pacing scores were significantly higher in ChR2 animals compared to control animals (4 Hz: $p < 0.01$, $Z = -4.7$, Wilcoxon Rank Sum Test; 8 Hz: $p < 0.01$, $Z = -3.5$, Wilcoxon Rank Sum Test; 12 Hz: $p < 0.01$, $Z = -6.3$, Wilcoxon Rank Sum Test).

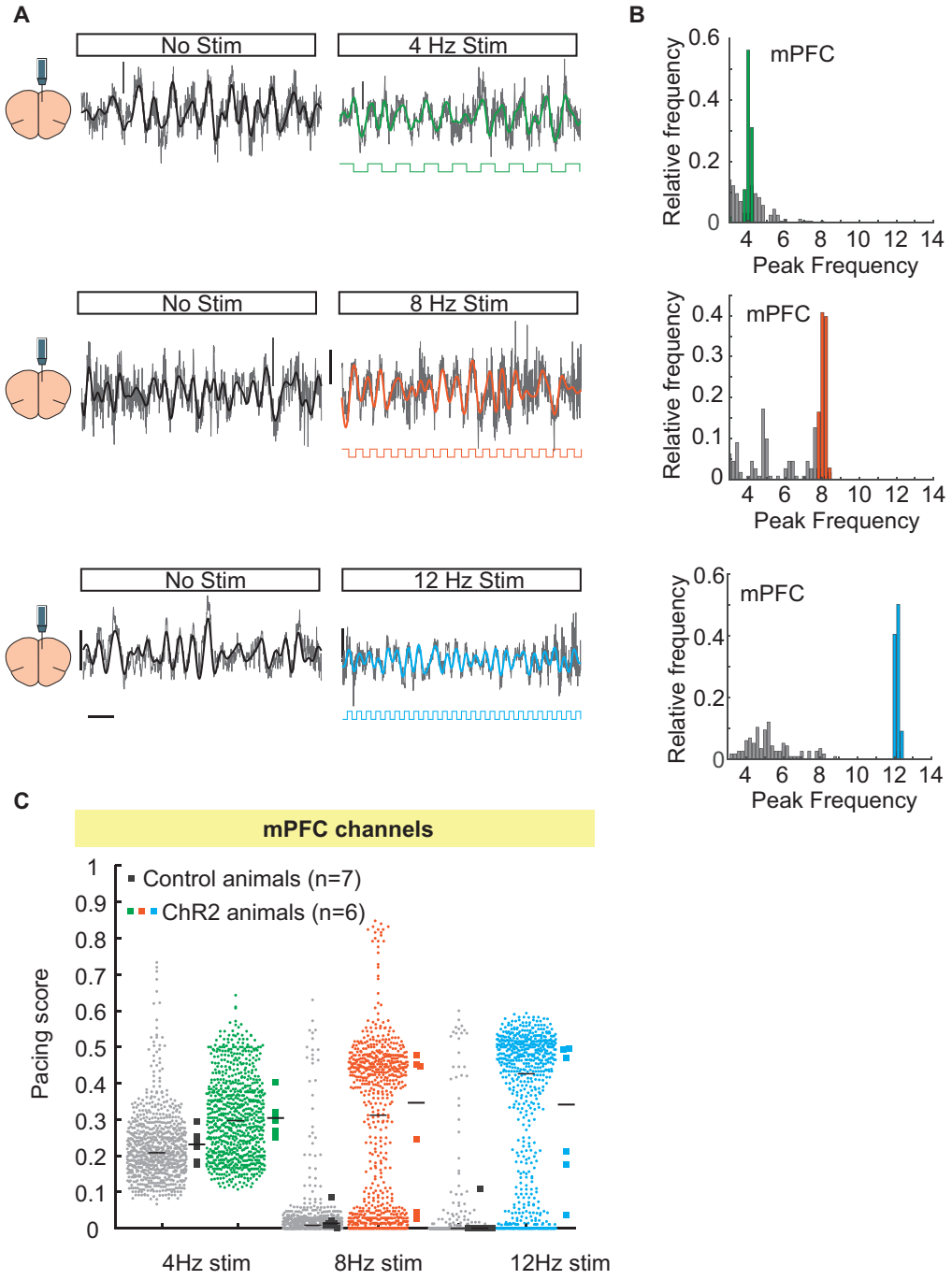

Figure 3. Optogenetic stimulation of MSA PV neurons paced mPFC LFP oscillations in a spatial alternation task. (A) mPFC LFP traces when 4Hz, 8Hz and 12Hz stimulation was turned on or off. Black and colored traces are filtered signals. Grey traces are unfiltered signals. Scale bar is 0.2 s. (B) Example histograms show the relative frequency of the predominant mPFC oscillation frequency in ChR2 animals when stimulation was turned on (colored) or off (grey). (C) Plots show the pacing score of mPFC channels in ChR2 animals (colored dots and squares) and control animals (grey dots and squares). Pacing scores are plotted both by sessions (dots) or as the average of all sessions and channels in an animals (squares).

The mPFC and HpC showed an increase in power at all stimulation frequencies and the power of ~4-5Hz oscillations in the mPFC was not altered with 8 Hz or 12 Hz optical stimulation in the MSA

To examine how mPFC and HpC oscillations are coordinated during stimulations, we recorded mPFC signals from 31 channels of a silicon probe and a hippocampal signal from a single electrode (Figure 9). When stimulation was turned off, endogenous oscillations at ~4 Hz were most prominent in the mPFC (Figure 4A). In the HpC, theta oscillations at ~8 Hz were most prominent (Figure 4B). However, when rhythmic optical stimulation was turned on, peak oscillations in both the mPFC and HpC shifted to the stimulation frequency (i.e. in figure 4A, when 4Hz stimulation was turned on, peak frequency in the mPFC shifted to 4Hz). Simultaneously, there was a decrease in the mPFC endogenous 8 Hz power during 4 Hz and 12Hz stimulations (Figure 4A).

To further understand how medial septal stimulation affected endogenous mPFC oscillations, we divided the mPFC oscillation frequency range into three bands, 3-5 Hz, 7-9 Hz and 11-13 Hz, and compared peak power in each band when stimulation was either on or off. The power in the 7-9 Hz band increased when 8 Hz stimulation was delivered to the MSA and decreased in response to 4 Hz and 12 Hz stimulation (4 Hz: $p = 0.046$, $Z = 2.52$, Wilcoxon Signed Rank Test; 8 Hz: $p < .01$ $Z = -4.5$, Wilcoxon Signed Rank Test; 12 Hz: $p < .01$, $Z = 4.1$, Wilcoxon Signed Rank Test, Figure 5A). This confirms that mPFC theta oscillations were controlled by medial septal stimulation. An increase in peak power in 3-5 Hz band was observed when 4 Hz stimulation was delivered to the MSA (4 Hz: $p < .01$, $Z = -4.2$, Wilcoxon Signed Rank Test). Interestingly, 8 Hz and 12 Hz medial septal stimulation did not decrease the power of the endogenous ~4-5 Hz oscillations (8 Hz: $p = 0.18$, $Z = 1.89$, Wilcoxon Signed Rank Test;

12 Hz: $p = 0.22$, $Z = -1.22$, Wilcoxon Signed Rank Test, Figure 5A), indicating that the ~4-5 Hz endogenous oscillation was not controlled by optical stimulation in the MSA. The 11-13 Hz band showed an increase in power with 12 Hz stimulation turned on, indicating mPFC LFP was paced by 12 Hz stimulation (12 Hz: $p < .01$, $Z = -4.6$, Wilcoxon Signed Rank Test, Figure 5A). Four Hz optical stimulation also increased power in the 11-13 Hz band but it is likely due to the emergence of harmonics ($p < .01$, $Z = -4.18$, Wilcoxon Signed Rank Test, Figure 5A). Similar to ChR2 animals, GFP control animals also showed an increase in power in the 7-9 Hz band in response to 8 Hz stimulation and an increase in power in the 11-13 Hz band in response to 12 Hz stimulation (8 Hz: $p = 0.03$, $Z = -2.9$, Wilcoxon Signed Rank Test, 12 Hz: $p < 0.01$, $Z = -3.7$, Wilcoxon Signed Rank Test). However, compared to ChR2 animals, these changes were slight and were perhaps due to heat generated by light stimulation or due to visual responses to the light stimulus (Figure 5A).

We conducted the same analyses on hippocampal LFP by examining peak power in 3-5 Hz, 7-9 Hz and 6-12 Hz band (Figure 5B). Four Hz stimulation led to an increase in power in the 3-5 Hz band, indicating HpC oscillations were paced at 4 Hz ($p < .01$, $Z = -4$, Wilcoxon Signed Rank Test). When 8 Hz and 12 Hz stimulation was turned on, peak power increased in the 7-9 Hz and 11-13 band, respectively (8 Hz: $p < 0.01$, $Z = -4.6$, Wilcoxon Signed Rank Test, 12 Hz: $p < 0.01$, $Z = -4.6$, Wilcoxon Signed Rank Test, Figure 5B). These findings confirmed successful pacing in the HpC by medial septal stimulation. All the changes in hippocampal LFP were observed only in ChR2 animals and not in GFP control animals (Figure 4B and Figure 5B).

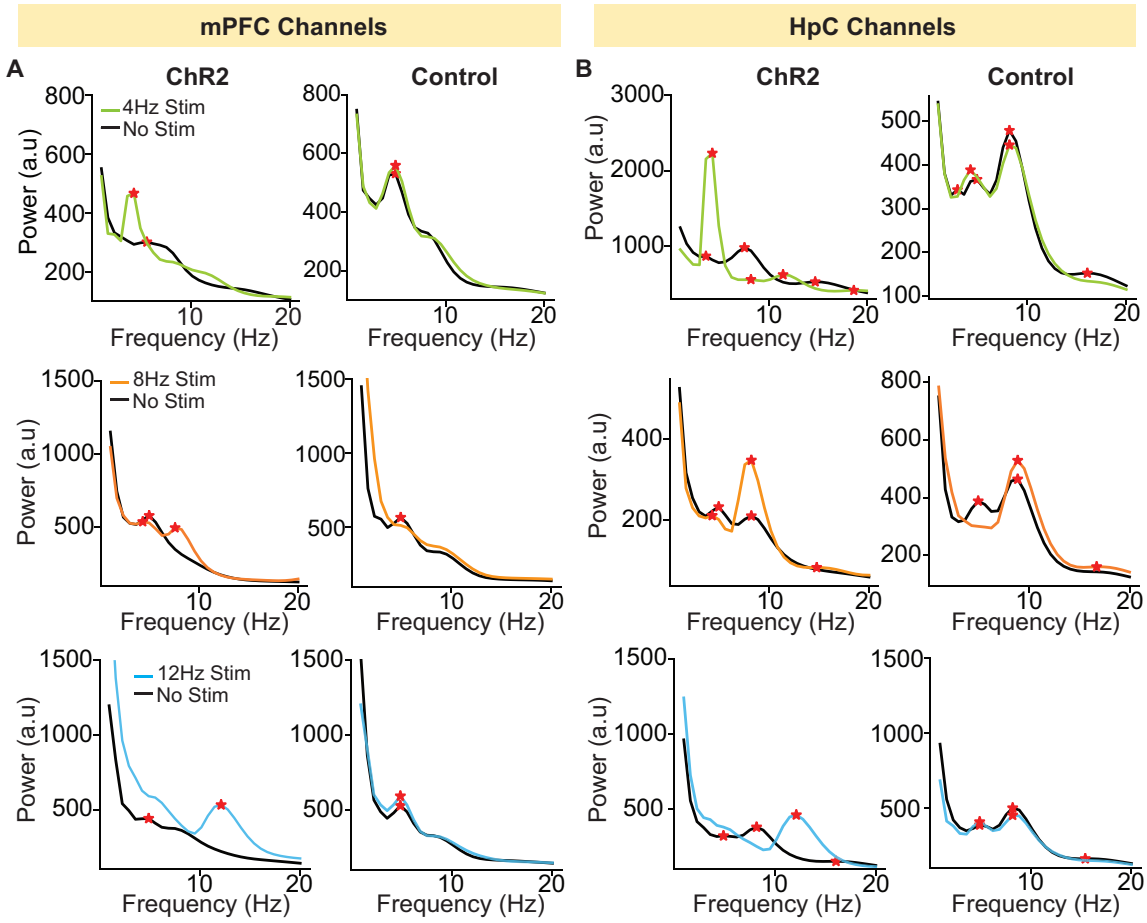

Figure 4. The mPFC and HpC LFP showed shifts in the predominant frequency so that the predominant frequency during stimulation corresponded to the stimulation frequencies. (A) Power spectra of mPFC LFP when stimulation was turned on (colored lines) or off (black lines) in ChR2 and control mice. Red asterisks represent peak frequencies in the power spectra. (B) Power spectra of the HpC LFP when stimulation was turned on (colored lines) or off (black lines) in ChR2 and control mice.

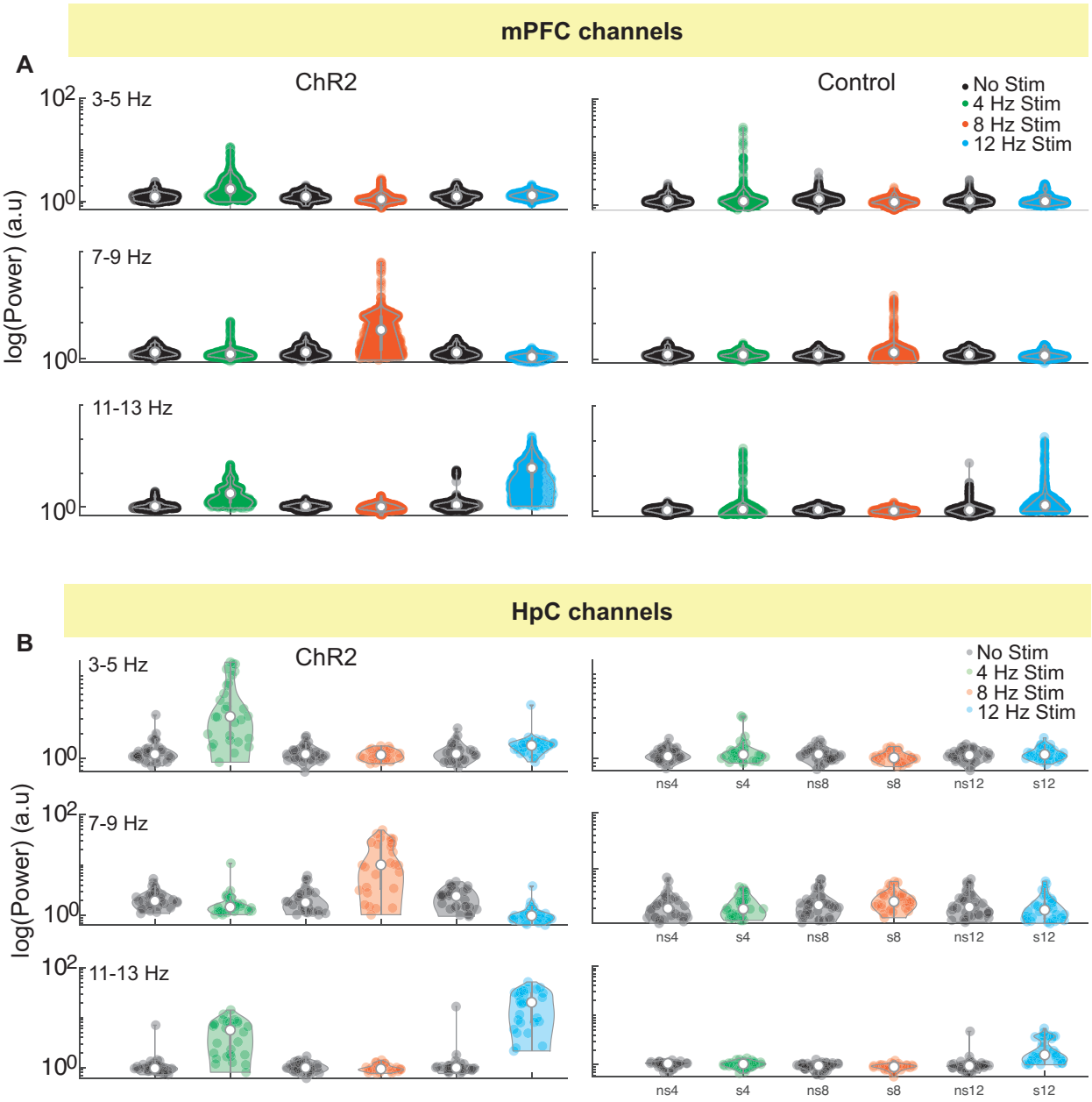

Figure 5. The power of endogenous mPFC 4 Hz oscillations was not altered by 8 Hz or 12 Hz optical stimulations. (A) mPFC peak power of ChR2 and control mice. Each dot represents one recording session. First row shows the peak power in the 3-5 Hz band. Middle row shows the peak power in the 7-9 Hz band. Bottom row shows the peak power in the 11-13 Hz band. (B) HpC peak power of ChR2 and control mice. Each dot represents one recording session. Top row shows the peak power in the 3-5 Hz band. Middle row shows the peak power in the 7-9 Hz band. Bottom row shows the peak power in the 11-13 Hz band.

mPFC-HpC coherence always increased at the stimulation frequency and 8 Hz and 12 Hz medial septal stimulation did not affect mPFC-HpC coherence of ~4-5 Hz oscillations

Based on the finding that mPFC and hippocampal oscillations were both paced by optical stimulation in the MSA, we hypothesized that oscillations across the two brain regions should also become more coherent. To analyze coherence, we generated coherence spectra between the hippocampal channel and each of the 31 recorded mPFC channels (Figure 10). When stimulation was turned off, there was a strong mPFC-HpC coherence at ~4-5 Hz and at the frequency of the endogenous theta oscillations (~ 8 Hz). However, when 4 Hz or 12 Hz stimulation was turned on, coherence decreased at 8 Hz but increased at the stimulation frequency. The mPFC-HpC coherence at 8 Hz was enhanced when 8 Hz stimulation was turned on (Figure 6A). Interestingly, during 8 Hz and 12 Hz stimulation, coherence at ~4-5 Hz remained unchanged compared to when stimulation was turned off (Figure 6A).

We further examined peak coherence in the 3-5 Hz, 7-9 Hz and 6-12 Hz band. When 4 Hz stimulation was delivered to the MSA, an increase in mPFC-HpC coherence was observed in the 3-5 Hz band (Figure 7A). However, the p value became slightly higher than 0.05 after Holm Bonferroni correction (4 Hz: $p = 0.059$, $Z = -2.4$, Wilcoxon Signed Rank Test), indicating the increase in mPFC-HpC coherence at 4 Hz oscillation was not significant. mPFC-HpC coherence in the 3-5 Hz band did not change upon 8 Hz or 12 Hz stimulation (8 Hz: $p = 0.28$, $Z = 1.5$, Wilcoxon Signed Rank Test; 12 Hz: $p = 0.73$, $Z = 0.3$, Wilcoxon Signed Rank Test). The increase in mPFC-HpC coherence in the 7-9 Hz band upon 8 Hz stimulation and decrease in coherence upon 4 Hz or 12 Hz stimulation suggest that the paced oscillations take control of the mechanism that otherwise controls endogenous theta oscillations (4 Hz: $p = 0.01$, $Z = 3.1$, Wilcoxon Signed Rank Test; 8 Hz: $p < .01$, $Z = -3.6$, Wilcoxon Signed Rank Test, 12 Hz: $p =$

0.02, Z = 2.9, Wilcoxon Signed Rank Test, Figure 7A). When 12 Hz stimulation was turned on, an increase in mPFC-HpC coherence was observed in the 11-13 Hz band in both ChR2 and control animals but the increase in control animals was smaller than that in ChR2 animals (ChR2: $p < .01$, $Z = -4.6$, Wilcoxon Signed Rank Test; control: $p < .01$, $Z = -4.5$, Wilcoxon Signed Rank Test, Figure 7, Figure 7A-B). We therefore conclude that mPFC-HpC coherence increased at all stimulation frequencies but that endogenous mPFC-HpC coherence at ~4-5 Hz remained unaffected with stimulation at the two higher frequencies (Figure 7A).

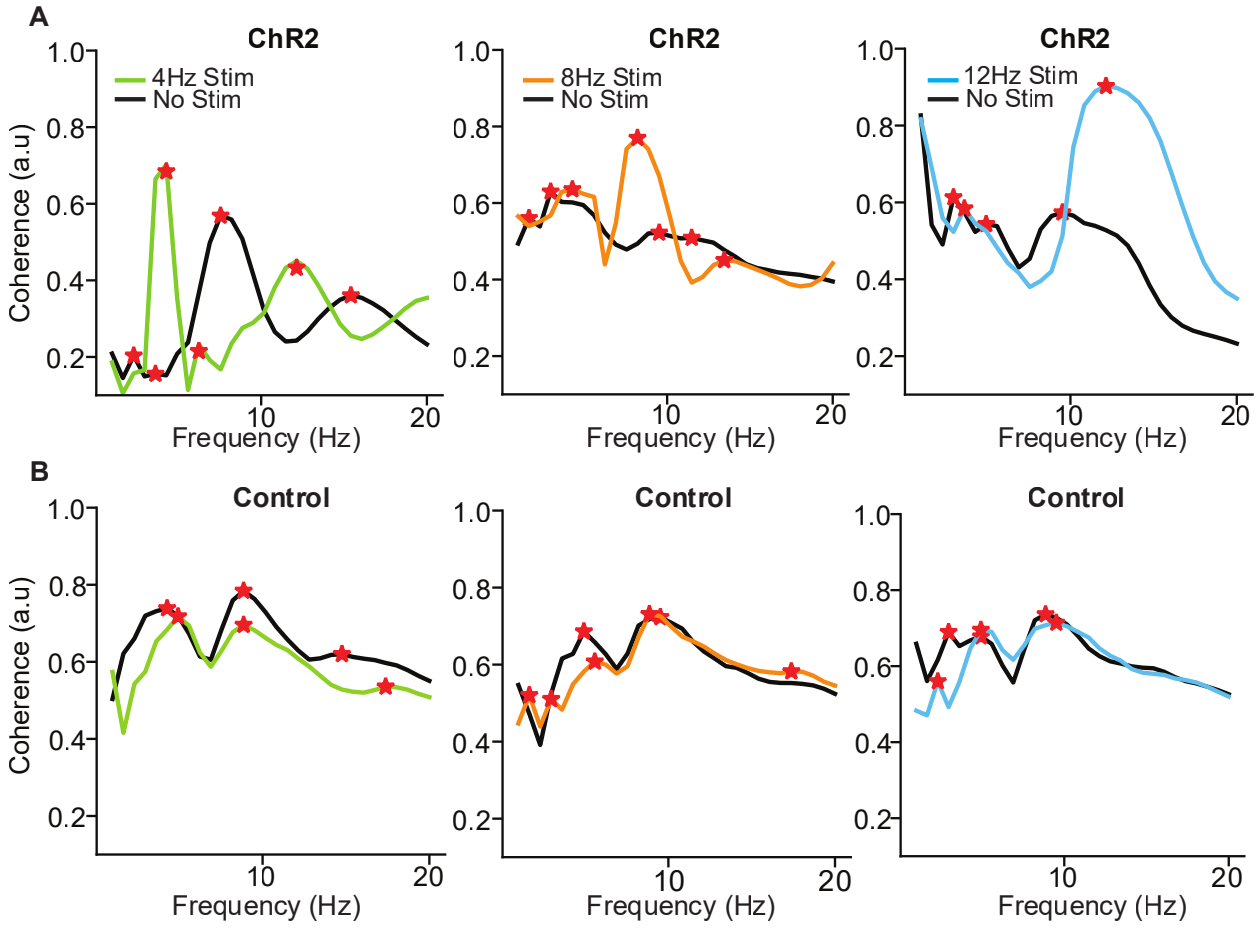

Figure 6. The mPFC showed strong coherence with the HpC at the stimulation frequencies. (A) Coherence spectra of mPFC-HpC LFP when stimulation was turned on (colored lines) or off (black lines) in ChR2 mice. Red asterisks represent peaks in the coherence spectra. (B) Coherence spectra of mPFC-HpC LFP when stimulation was turned on (colored lines) or off (black lines) in control mice.

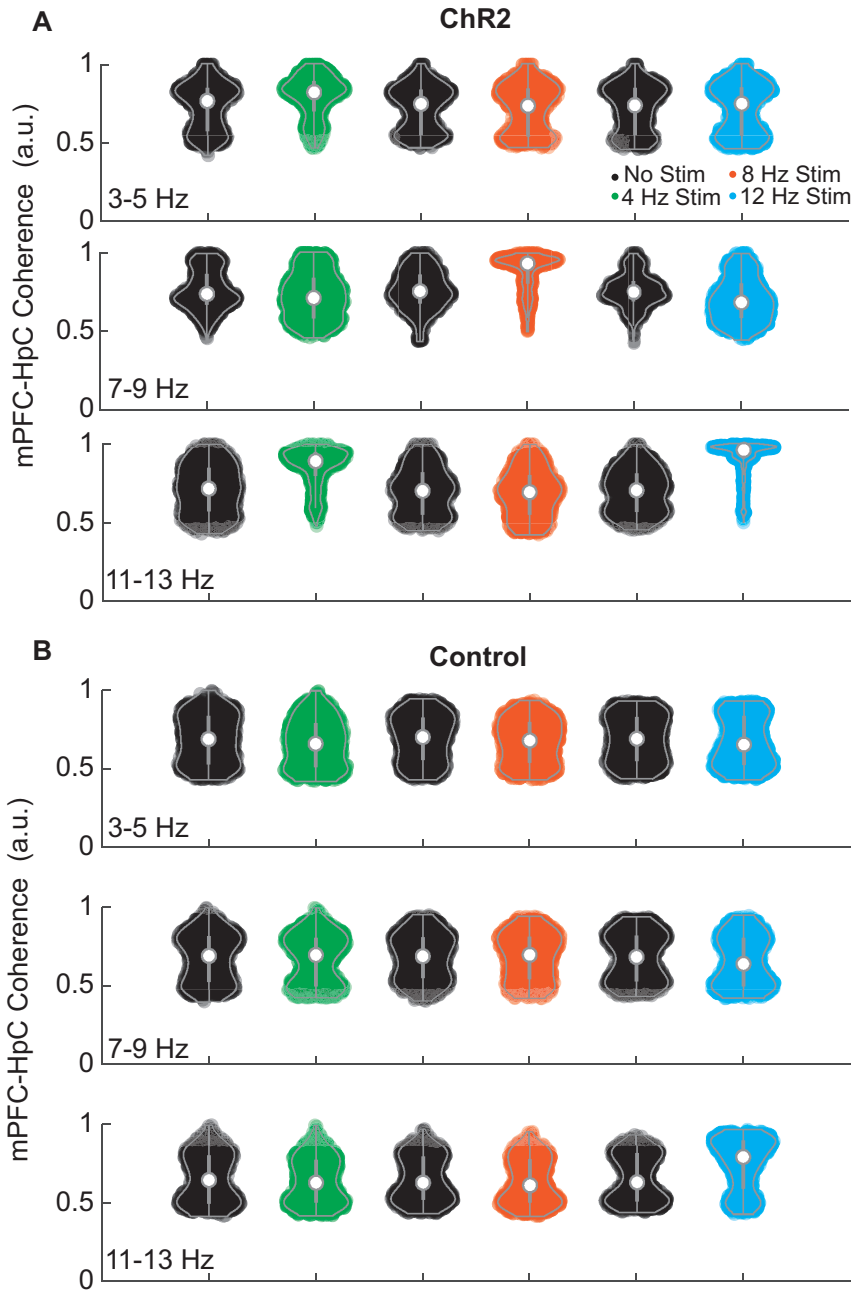

Figure 7. mPFC-HpC coherence at 4 Hz was not affected by 8 Hz or 12 Hz stimulation in the MSA. (A) Coherence between mPFC and hippocampal LFP in ChR2 mice when stimulation was turned on (colored) or off (black). Top row shows the peak coherence in the 3-5 Hz band. Middle row shows the peak coherence in the 7-9 Hz band. Bottom row shows the peak coherence in the 11-13 Hz band. (B) Coherence between mPFC and hippocampal LFP in control mice when stimulation was turned on (colored) or off (black). Top row shows the peak coherence in the 3-5 Hz band. Middle row shows the peak coherence in the 7-9 Hz band. Bottom row shows the peak coherence in the 11-13 Hz band.

Optical stimulation in the MSA did not cause behavioral changes in a spatial alternation task

As described in the methods section, both ChR2 and control mice performed a figure-8 maze alternation task with stimulation turned on every other block (10 trials) (Figure 2A-B). Each animal underwent 15 recording sessions with 5 sessions for each the three stimulation frequencies (4 Hz, 8 Hz and 12 Hz). The performance of each animal for each delay condition (0s, 2s and 10s) was averaged across all recording sessions of the same stimulation frequency. T-tests were used to compare the difference in performance accuracy between trials with stimulation turned on and trials with stimulation turned off. Holm-Bonferroni correction was performed to correct multiple comparisons. In the no delay, 2 second delay and 10 second delay versions of the task, performance accuracy of mice that expressed ChR2 did not differ between trials with stimulation turned on or off (Figure 8A and Table 2). Behavioral performance of control animals was not affected by stimulation of any frequencies in any delay interval (Figure 8A and Table 3). To further quantify how stimulation at different frequencies affected the animals' performance, we calculated the change in performance between no stimulation and stimulation trials. Change in performance was compared between ChR2 and control animals across all delay intervals and all stimulation frequencies (Figure 8B). No significant effects were found for the change in performance between no-stimulation and stimulation trials.

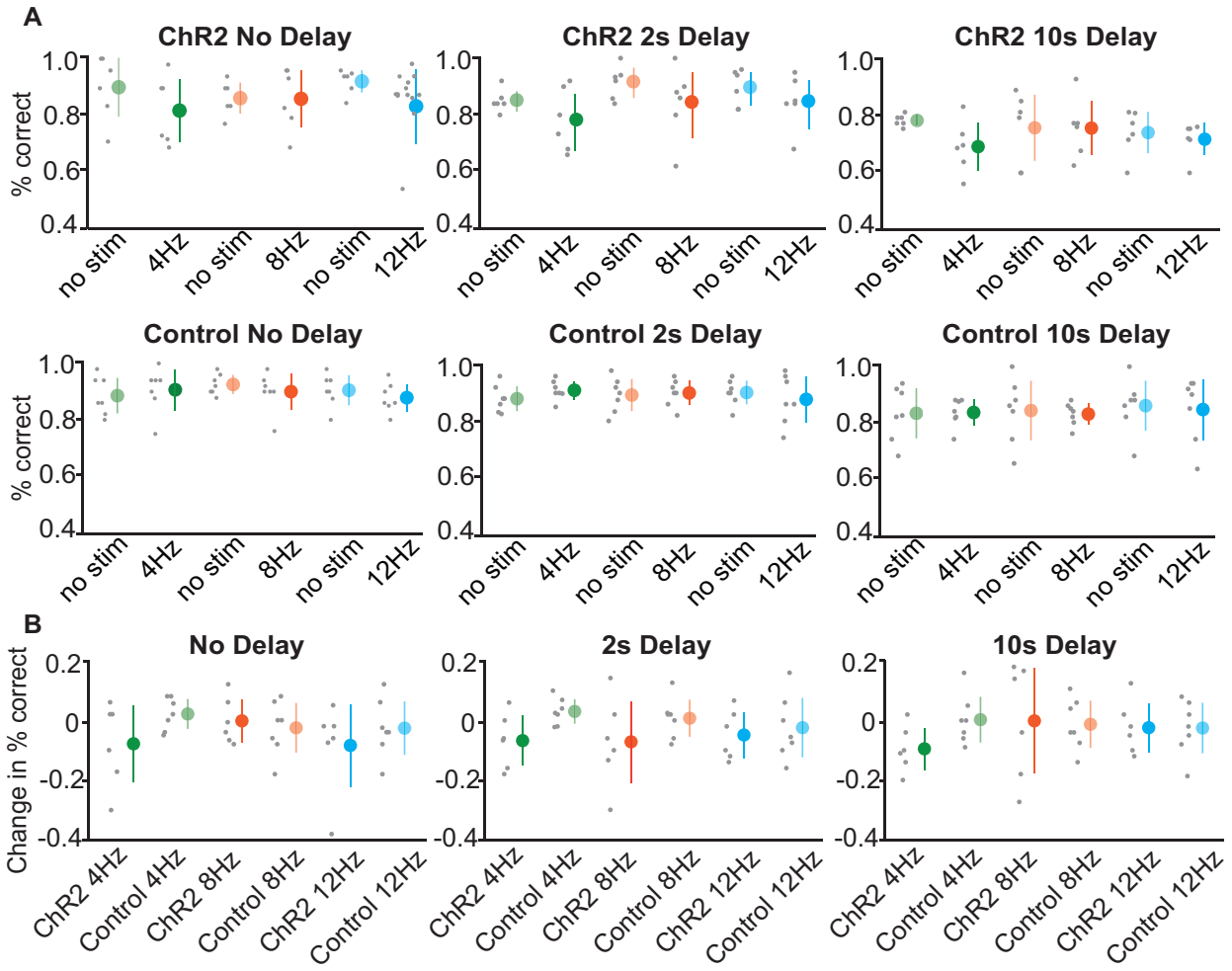

Figure 8. In our cohort of mice, no effects on behavior by septal stimulation were detected. (A) Performance accuracy of ChR2 and control mice in the alternation task during trials with no delay, 2-s delay, and 10-s delay with or without optical stimulations. Each grey dot represents the average performance of one mouse during trials with either stimulation turned on or off and with no delay, 2-s delay, or 10-s delay (n=6 for ChR2 and n=7 for control). Colored dots represent the average for each condition, and colored bars represent standard deviation. (B) Change in performance accuracy of ChR2 and control mice between no-stimulation and stimulation trials. The different delay conditions are plotted separately. Positive values indicate behavioral improvements with stimulation turned on and negative values indicate behavioral impairments with stimulation turned on. Each grey dot represents the change in performance of each animal, colored dots represent the average change in performance for each animal, and colored bars represent the standard deviation.

Table 2. Statistical analysis of ChR2 animals' performance across all frequencies and delays. Paired t-tests were performed on the performance of ChR2 animals (n=6). Holm-Bonferroni correction was used to correct the p values obtained from the paired t-tests. Corrected p values showed no significance.

	Holm-Bonferroni correction, p values		
	4 Hz n = 6	**8 Hz n = 6**	**12 Hz n = 6**
No delay	0.22	0.94	0.23
2s delay	0.13	0.29	0.21
10s delay	0.26	0.99	0.54

Table 3. Statistical analysis of control animals' performance across all frequencies and delays. Paired t-tests were performed on the performance of control animals (n=7). P values showed no significance.

	Paired t-test, p values		
	4 Hz n = 7	**8 Hz n = 7**	**12 Hz n = 7**
No delay	0.34	0.48	0.49
2s delay	0.12	0.78	0.57
10s delay	0.93	0.71	0.72

CHAPTER III: DISCUSSION

Hippocampal theta oscillations (7-9 Hz) are known to be the most prominent oscillatory pattern in the HpC and play an important role in mediating neuronal activities across different brain regions to support spatial working memory (Mitchell et al., 1982; O'Neill et al., 2013). Besides HpC, mPFC is also crucial for working memory and has been shown to support working memory in the absence of HpC via a compensatory mechanism (Yang, 2014; Lee and Kesner, 2003). Both mPFC and HpC exhibit prominent theta oscillations in working memory while mPFC also shows strong endogenous ~4-5 Hz oscillations (O'Neill et al., 2013; Fijisawa and Buzsaki., 2011). In our study, we manipulated hippocampal theta oscillations via optical stimulation in the MSA and explored how that affected mPFC theta oscillations in a figure-8 maze spatial alternation task. We first calculated the hippocampal and prefrontal pacing scores which were significantly higher in ChR2 injected animals than in control animals (Figure 2E and 3C). This indicated that both mPFC and hippocampal theta oscillations were paced by optical stimulation in the MSA. Furthermore, both HpC and mPFC LFP showed an increase in power at all stimulation frequencies, while power at 8 Hz was often decreased when stimulating at either a higher or lower frequency. However, neither 8 Hz nor 12 Hz stimulation changed the power of the endogenous ~4-5 Hz oscillations in the mPFC (Figure 5). In addition, mPFC showed strong coherence with the HpC at the stimulation frequency while the mPFC-HpC coherence at the endogenous ~4-5 Hz oscillations remained unaffected by 8 Hz or 12 Hz stimulation (Figure 7). Lastly, we examined whether optical stimulation in the MSA affected performance in a working memory task and observed no significant change in performance (Figure 8).

HpC and mPFC were paced by MSA optical stimulation

Optogenetic control of GABAergic parvalbumin- positive medial septal neurons gives rise to reliable pacing of hippocampal theta oscillations (Mitchell et al., 1982; Zutshi et al., 2018). Because of the reported anatomical and physiological connections between HpC and mPFC, we asked whether optical stimulation in the MSA also modulates mPFC theta oscillations (Shaw and Aggelton., 1993; Rajasethupathy et al., 2015; Dolorfo and Amaral, 1998). We found that HpC and mPFC theta oscillations both shifted to the stimulation frequency, suggesting both brain regions were paced by stimulation in the MSA (Figure 2C and 3A). To examine the extent of pacing, we calculated the pacing score for each animal, and ChR2 injected animals exhibited significantly higher pacing scores than control animals (Figure 2D-E and 3B-C). Given the effectiveness of pacing across brain regions, our findings therefore show that optical stimulation of PV-positive neurons in the MSA not only paced hippocampal, but also prefrontal theta oscillations (Figure 2-3). We hypothesize that there are two possible mechanisms by which mPFC is paced by MSA: direct pacing in mPFC by MSA or indirect pacing by MSA through HpC projections to mPFC. Anatomical studies have revealed that although the infralimbic subregion of the mPFC receives direct projections from the MSA, medial septal projections predominantly target the hippocampal regions (Gaykema et al., 1990; Kummer et al., 2020). Therefore, it is more likely that mPFC is indirectly paced by MSA via mPFC-HpC projections.

mPFC and hippocampal oscillations showed increase in power at stimulation frequencies where strong hippocampal-prefrontal coherence was also observed

Based on our finding that both HpC and mPFC LFP were paced by septal stimulation, we examined how the power of mPFC and hippocampal oscillations changed when stimulation was

on. As expected, mPFC and hippocampal LFP showed an increase in power at the stimulation frequency, further confirming the successful pacing of mPFC and hippocampal LFP by optical stimulation in the MSA (Figure 4-5). Additionally, we explored whether the paced mPFC and hippocampal LFP oscillated together. Coherence spectra between the mPFC and HpC exhibited the highest coherence at the stimulation frequency, indicating mPFC and HpC were paced and coherent at the stimulation frequency (Figure 6-7).

Endogenous ~4-5Hz oscillations in the mPFC remained unaffected by 8 Hz or 12 Hz optical stimulation in the MSA

MSA has been shown to be the pacemaker of hippocampal theta oscillations, meaning it not only adds a new oscillation at the stimulation frequency but also decreases the ongoing, endogenous oscillations in the HpC (Zutshi et al., 2018). We found that MSA also acts as a pacemaker of mPFC theta oscillations, indicated by an increase in power and mPFC-HpC coherence at all stimulation frequencies (4 Hz, 8 Hz, 12 Hz) and a reduction in power and mPFC-HpC coherence at ~8 Hz when 4 Hz or 12 Hz stimulation was turned on (Figure 4 and 6). Interestingly, we found that the power of the endogenous ~4-5 Hz oscillations in the mPFC and their coherence with hippocampal oscillations remained unaffected by 8 Hz or 12 Hz stimulation in the MSA (Figure 5 and Figure 7A). This indicates that these ~4-5 Hz oscillations are not paced by optical stimulation in the MSA and may have a different mechanism of generation from endogenous theta oscillations (i.e. respiratory rhythm). The endogenous 4 Hz oscillations in prefrontal cortex have been found to exhibit a prominent increase in power and coherence between prefrontal cortex and ventral tegmental area in a working memory task (Fujisawa and Buzaki, 2011). Therefore, future experiments could explore what generates or paces the ~4-5 Hz

oscillations in mPFC and whether these oscillations contribute to the prefrontal compensatory mechanism in working memory when the HpC is absent.

Optical stimulation in the MSA did not cause behavioral improvements or impairments in a figure-8 maze alternation task

We used a figure-8 maze alternation task to assess working memory. The task has been shown to be HpC independent when no delay is used (Wood et al., 2000). Accordingly, we found that the accuracy of mice that performed the continuous alternation task (i.e., with no delay) was not affected by optical stimulation delivered to the MSA. Previous findings showed that HpC becomes more important for working memory when delays are interposed in the task. (Sabariego et al., 2019; Ainge et al., 2007). To examine whether pacing hippocampal oscillations would affect working memory performance, we made the task HpC dependent by adding 2-second and 10-second delays. However, stimulation in the MSA did not cause significant behavioral changes in task versions with delay (Figure 8). A previous study has shown behavioral improvements with 4 Hz stimulation and behavioral impairments with 12 Hz stimulation in the 10-second delay version of a figure-8 maze spatial alternation task (Devico et al., 2020). The discrepancy in our findings could be due to the difference in sample size and number of recording sessions. In our study, we only included 6 ChR2 animals and 7 control GFP animals with 15 recording sessions for each animal while Devico et al. included 12 ChR2 animals and 4 control animals with 10 recording sessions for each animal. In addition, in the Devico et al. study, delays were first introduced to the task after the animals underwent the mPFC implantation surgery while in our study, delays were introduced to the task before the animals underwent the implantation surgery.

The different timing of when delays were introduced to the task could affect how well the animals mastered the task and account for the difference in performance accuracy as well.

CHAPTER IV: CONCLUSION

We confirmed that hippocampal theta oscillations can be effectively paced by optical stimulation in the MSA, as shown by an increase in power at the stimulation frequency. The effectiveness of pacing was quantified by calculating pacing scores, and ChR2 animals exhibited significantly higher pacing scores than GFP control animals. Similar to the effects on hippocampal theta, we observed that mPFC theta oscillations were effectively manipulated by medial septal stimulation. The oscillations in mPFC responded to the stimulation with an increase in power and an increase in coherence with the HpC LFP. Again, ChR2 animals exhibited higher pacing scores than control animals. These results demonstrate that theta oscillations in the mPFC and HpC were each paced by MSA stimulation and were paced coherently with each other. Furthermore, we found that the power of the mPFC endogenous ~4-5 Hz oscillations and their coherence with the HpC were not modulated by stimulation at 8 Hz and 12 Hz. This is an indication that the ~4-5 Hz oscillations in the mPFC were not superseded by oscillations that were driven by MSA stimulation, suggesting that these oscillations are driven by a different mechanism than the canonical theta oscillations (e.g., the respiratory rhythm). In addition, we also examined whether MSA stimulation affected working memory performance. Our data showed no behavioral improvements or impairments caused by optical stimulation in the MSA, but it is possible that the current studies were not powered to detect behavioral effects.

This thesis is currently being prepared for submission of publication of the material by Srikanth, Sunandha.; Hu, Yudi.; Leutgeb, Jill K.; Leutgeb, Stefan. The author of this thesis will be a co-author of the publication.

APPENDIX FIGURES

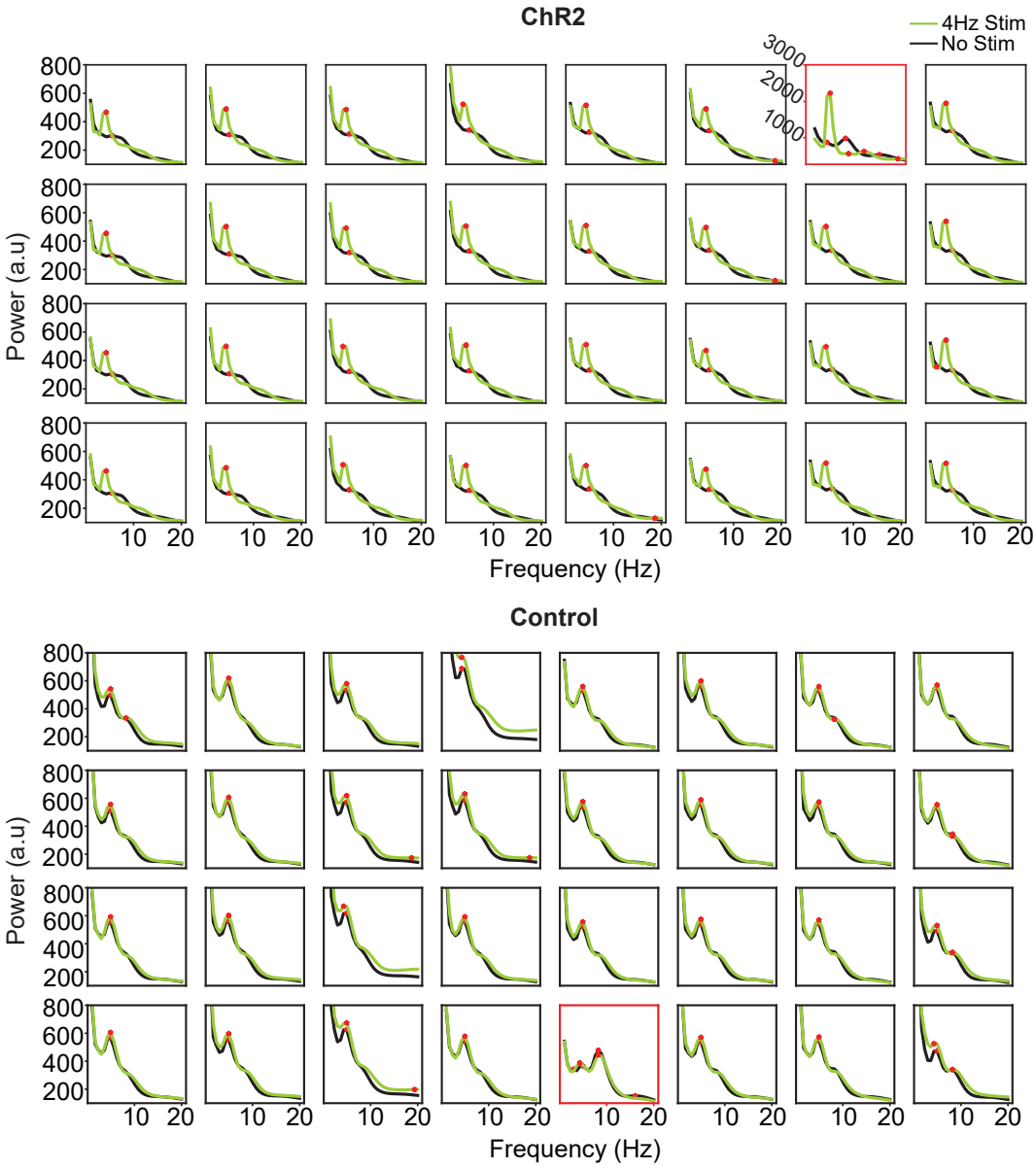

Figure 9. Example power spectra of all 32 recording channels in a 4Hz stimulation session. Power spectra of mPFC and hippocampal LFP when 4Hz stimulation was turned on (green lines) and off (black lines) in a ChR2 and a control animal. Red asterisks represent peak frequencies in the power spectra. Hippocampal channels are indicated by red boxes.

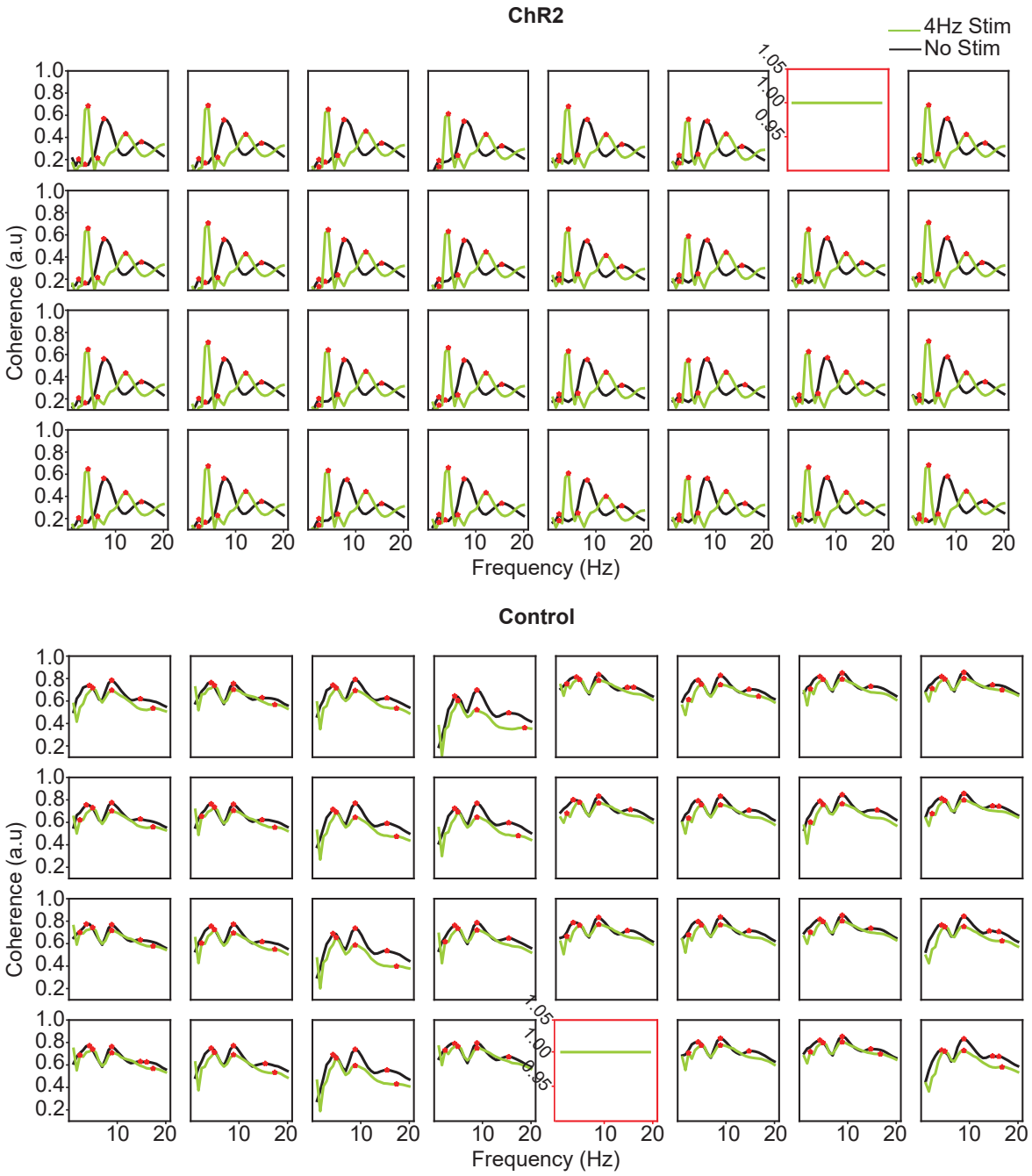

Figure 10. Example coherence spectra of all 31 mPFC channels in a 4Hz stimulation session. Coherence spectra between mPFC and hippocampal LFP when 4Hz stimulation was turned on (green lines) and off (black lines) in a ChR2 and a control animal. Red asterisks represent peak frequencies in the coherence spectra. The hippocampal channel (in the red box) has a coherence of 1.

REFERENCES

Ainge, J. A., van der Meer, M. A., Langston, R. F., & Wood, E. R. (2007). Exploring the role of context-dependent hippocampal activity in spatial alternation behavior. *Hippocampus*, *17*(10), 988–1002. https://doi.org/10.1002/hipo.20301

Amaral, D. G., & Witter, M. P. (1989). The three-dimensional organization of the hippocampal formation: a review of anatomical data. *Neuroscience*, *31*(3), 571–591. https://doi.org/10.1016/0306-4522(89)90424-7

Backus, A. R., Schoffelen, J.-M., Szebényi, S., Hanslmayr, S., & Doeller, C. F. (2016). Hippocampal-Prefrontal Theta Oscillations Support Memory Integration. *Current Biology*, *26*(4), 450–457. https://doi.org/10.1016/j.cub.2015.12.048

Baddeley A. (1992). Working memory. *Science (New York, N.Y.)*, *255*(5044), 556–559. https://doi.org/10.1126/science.1736359

Brincat, S. L., & Miller, E. K. (2015). Frequency-specific hippocampal-prefrontal interactions during associative learning. *Nature neuroscience*, *18*(4), 576–581. https://doi.org/10.1038/nn.3954

Colgin L. L. (2011). Oscillations and hippocampal-prefrontal synchrony. *Current opinion in neurobiology*, *21*(3), 467–474. https://doi.org/10.1016/j.conb.2011.04.006

Devico, N. (2020). *Accelerating and decelerating hippocampal theta oscillations via optogenetic stimulations has opposing effects on spatial working memory.* (Unpublished master's thesis). University of California San Diego, San Diego, California, United States.

Dickerson, B. C., & Eichenbaum, H. (2010). The episodic memory system: neurocircuitry and disorders. *Neuropsychopharmacology : official publication of the American College of Neuropsychopharmacology*, *35*(1), 86–104. https://doi.org/10.1038/npp.2009.126

Dolorfo, C. L., & Amaral, D. G. (1998). Entorhinal cortex of the rat: topographic organization of the cells of origin of the perforant path projection to the dentate gyrus. *The Journal of comparative neurology*, *398*(1), 25–48.

Eichenbaum H. (2000). A cortical-hippocampal system for declarative memory. *Nature reviews. Neuroscience*, *1*(1), 41–50. https://doi.org/10.1038/35036213

Frank, L. M., Brown, E. N., & Wilson, M. (2000). Trajectory encoding in the hippocampus and entorhinal cortex. Neuron, 27(1), 169–178. https://doi.org/10.1016/s0896 6273(00)00018-0

Fries, P. (2009). Neuronal Gamma-Band Synchronization as a Fundamental Process in Cortical Computation. *Annual Review of Neuroscience*, *32*(1), 209–224. https://doi.org/10.1146/annurev.neuro.051508.135603

Fujisawa, S., & Buzsáki, G. (2011). A 4 Hz oscillation adaptively synchronizes prefrontal, VTA, and hippocampal activities. *Neuron*, *72*(1), 153–165. https://doi.org/10.1016/j.neuron.2011.08.018

Gaykema, R. P., Luiten, P. G., Nyakas, C., & Traber, J. (1990). Cortical projection patterns of the medial septum-diagonal band complex. The Journal of comparative neurology, 293(1), 103–124. https://doi.org/10.1002/cne.902930109

Hannesson, D. K., Vacca, G., Howland, J. G., & Phillips, A. G. (2004). Medial prefrontal cortex is involved in spatial temporal order memory but not spatial recognition memory in tests relying on spontaneous exploration in rats. *Behavioural brain research*, *153*(1), 273–285. https://doi.org/10.1016/j.bbr.2003.12.004

Ji, G., & Neugebauer, V. (2012). Modulation of medial prefrontal cortical activity using in vivo recordings and optogenetics. *Molecular brain*, *5*, 36. https://doi.org/10.1186/1756-6606-5-36

Kummer, K. K., Mitrić, M., Kalpachidou, T., & Kress, M. (2020). The Medial Prefrontal Cortex as a Central Hub for Mental Comorbidities Associated with Chronic Pain. *International Journal of Molecular Sciences*, *21*(10), 3440. https://doi.org/10.3390/ijms21103440

Lee, I., & Kesner, R. P. (2003). Time-dependent relationship between the dorsal hippocampus and the prefrontal cortex in spatial memory. *The Journal of neuroscience : the official journal of the Society for Neuroscience*, *23*(4), 1517–1523. https://doi.org/10.1523/JNEUROSCI.23-04-01517.2003

Milner, B., Corkin, S., & Teuber, H.-L. (1968). Further analysis of the hippocampal amnesic syndrome: 14-year follow-up study of H.M. *Neuropsychologia*, *6*(3), 215–234. https://doi.org/10.1016/0028-3932(68)90021-3

Mitchell, S. J., Rawlins, J. N., Steward, O., & Olton, D. S. (1982). Medial septal area lesions disrupt theta rhythm and cholinergic staining in medial entorhinal cortex and produce impaired radial arm maze behavior in rats. *The Journal of neuroscience : the official journal of the Society for Neuroscience*, *2*(3), 292–302. https://doi.org/10.1523/JNEUROSCI.02-03-00292.1982

Morris, R. G., Garrud, P., Rawlins, J. N., & O'Keefe, J. (1982). Place navigation impaired in rats with hippocampal lesions. *Nature*, *297*(5868), 681–683. https://doi.org/10.1038/297681a0

O'Keefe, J., & Recce, M. L. (1993). Phase relationship between hippocampal place units and the EEG theta rhythm. *Hippocampus*, *3*(3), 317–330. https://doi.org/10.1002/hipo.450030307

O'Neill, P. K., Gordon, J. A., & Sigurdsson, T. (2013). Theta oscillations in the medial prefrontal cortex are modulated by spatial working memory and synchronize with the hippocampus through its ventral subregion. *The Journal of neuroscience : the official journal of the*

Society for Neuroscience, *33*(35), 14211–14224. https://doi.org/10.1523/JNEUROSCI.2378-13.2013

Poucet, B., & Buhot, M. C. (1994). Effects of medial septal or unilateral hippocampal inactivations on reference and working spatial memory in rats. *Hippocampus*, *4*(3), 315–321. https://doi.org/10.1002/hipo.450040315

Rajasethupathy, P., Sankaran, S., Marshel, J. H., Kim, C. K., Ferenczi, E., Lee, S. Y., Berndt, A., Ramakrishnan, C., Jaffe, A., Lo, M., Liston, C., & Deisseroth, K. (2015). Projections from neocortex mediate top-down control of memory retrieval. *Nature*, *526*(7575), 653–659. https://doi.org/10.1038/nature15389

Reed, J. M., & Squire, L. R. (1998). Retrograde amnesia for facts and events: findings from four new cases. The Journal of neuroscience : the official journal of the Society for Neuroscience, 18(10), 3943–3954. https://doi.org/10.1523/JNEUROSCI.18-10 03943.1998

Rossi, M. A., Hayrapetyan, V. Y., Maimon, B., Mak, K., Je, H. S., & Yin, H. H. (2012). Prefrontal cortical mechanisms underlying delayed alternation in mice. *Journal of neurophysiology*, *108*(4), 1211–1222. https://doi.org/10.1152/jn.01060.2011

Sabariego, M., Schönwald, A., Boublil, B. L., Zimmerman, D. T., Ahmadi, S., Gonzalez, N., Leibold, C., Clark, R. E., Leutgeb, J. K., & Leutgeb, S. (2019). Time Cells in the Hippocampus Are Neither Dependent on Medial Entorhinal Cortex Inputs nor Necessary for Spatial Working Memory. *Neuron*, *102*(6), 1235–1248.e5. https://doi.org/10.1016/j.neuron.2019.04.005

Scoville, W. B., & Milner, B. (2000). Loss of recent memory after bilateral hippocampal lesions. 1957. *The Journal of neuropsychiatry and clinical neurosciences*, *12*(1), 103–113. https://doi.org/10.1176/jnp.12.1.103

Shaw, C., & Aggleton, J. P. (1993). The effects of fornix and medial prefrontal lesions on delayed non-matching-to-sample by rats. *Behavioural brain research*, *54*(1), 91–102. https://doi.org/10.1016/0166-4328(93)90051-q

Siapas, A. G., Lubenov, E. V., & Wilson, M. A. (2005). Prefrontal phase locking to hippocampal theta oscillations. *Neuron*, *46*(1), 141–151. https://doi.org/10.1016/j.neuron.2005.02.028

Squire L. R. (2009). The legacy of patient H.M. for neuroscience. *Neuron*, *61*(1), 6–9. https://doi.org/10.1016/j.neuron.2008.12.023

Squire, L. R., & Zola-Morgan, S. (1991). The medial temporal lobe memory system. *Science (New York, N.Y.)*, *253*(5026), 1380–1386. https://doi.org/10.1126/science.1896849

Tehovnik, E. J., & Sommer, M. A. (1997). Effective spread and timecourse of neural inactivation caused by lidocaine injection in monkey cerebral cortex. *Journal of neuroscience methods*, *74*(1), 17–26. https://doi.org/10.1016/s0165-0270(97)02229-2

Tse, D., Langston, R. F., Kakeyama, M., Bethus, I., Spooner, P. A., Wood, E. R., Witter, M. P., & Morris, R. G. (2007). Schemas and memory consolidation. *Science (New York, N.Y.)*, *316*(5821), 76–82. https://doi.org/10.1126/science.1135935

Vanderwolf C. H. (1969). Hippocampal electrical activity and voluntary movement in the rat. *Electroencephalography and clinical neurophysiology*, *26*(4), 407–418. https://doi.org/10.1016/0013-4694(69)90092-3

Winson J. (1978). Loss of hippocampal theta rhythm results in spatial memory deficit in the rat. *Science (New York, N.Y.)*, *201*(4351), 160–163. https://doi.org/10.1126/science.663646

Wood ER, Dudchenko PA, Robitsek RJ, Eichenbaum H. Hippocampal neurons encode information about different types of memory episodes occurring in the same location. *Neuron*. 2000;27(3):623-633. doi:10.1016/s0896-6273(00)00071-4

Yang, S.-T., Shi, Y., Wang, Q., Peng, J.-Y., & Li, B.-M. (2014). Neuronal representation of working memory in the medial prefrontal cortex of rats. *Molecular Brain*, *7*(1). https://doi.org/10.1186/s13041-014-0061-2

Zutshi, I., Brandon, M. P., Fu, M. L., Donegan, M. L., Leutgeb, J. K., & Leutgeb, S. (2018). Hippocampal Neural Circuits Respond to Optogenetic Pacing of Theta Frequencies by Generating Accelerated Oscillation Frequencies. *Current biology : CB*, *28*(8), 1179–1188.e3. https://doi.org/10.1016/j.cub.2018.02.061